Proceedings of the 6th International
Conference on Chemical Vapor Deposition,
Atlanta, GA, October 10 - 13, 1977

LBL-6902

NUMERICAL SIMULATION OF TRANSPORT PROCESSES IN VERTICAL CYLINDER EPITAXY REACTORS

Charles W. Manke and Lee F. Donaghey

August 1977

Prepared for the U. S. Energy Research and
Development Administration under Contract W-7405-ENG-48

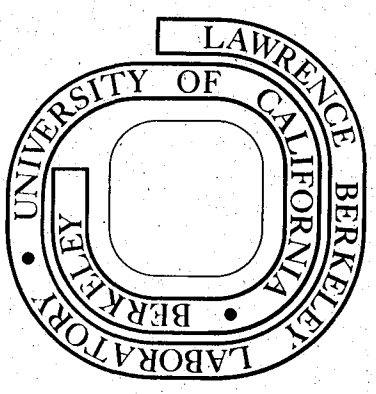

NUMERICAL SIMULATION OF TRANSPORT PROCESSES IN VERTICAL CYLINDER EPITAXY REACTORS

Charles W. Manke and Lee F. Donaghey*
Materials and Molecular Research Div., Lawrence Berkeley Laboratory
and Department of Chemical Engineering, University of California,
Berkeley, California 94720

A numerical method employing a marching integration, finite difference method is used to determine the momentum, temperature, and component molar concentration profiles in the tapered annulus of a vertical cylinder epitaxy reactor for silicon deposition from $SiCl_4$ in H_2. Results of the study contribute to the understanding of momentum, heat, and mass transfer in the vertical cylinder reactor. The numerical results indicate that boundary layers control the deposition profile in the entrance length of the reactor, while downstream rates are governed by the inlet flow rate and susceptor tilt angle.

INTRODUCTION

The exploration of transport processes occuring in chemical vapor deposition reactors for the epitaxial growth of silicon from tetrachlorosilane in hydrogen has received considerable attention in the literature, both for the purpose of reactor design and scale-up, and for an improved understanding of experimental phenomena. Models for the epitaxial growth of silicon in small horizontal CVD reactors have been developed by many authors. Shepherd developed an expression for the deposition rate as a function of distance along the reactor flow channel by assuming a parabolic velocity profile and a linear temperature gradient.[1] Eversteijn and Peek assumed that the flow channel could be divided into equal zones in stagnant and turbulent flow to develop a similar growth rate equation.[2,3] Rundle's model assumes an isothermal gas and a laminar gas velocity distribution.[4,5]

The advent of the vertical cylinder reactor has allowed a significant increase in the substrate capacity over the horizontal reactors.[6] Both Fujii et al.[7] and Dittman[8] have proposed models for the distribution of the deposition rate in the vertical cylinder reactor based on experimental data. In all of the above models, the variation of growth rate with position along the susceptor is determined by the extent of reactant depletion in the flow channel, and some transport processes are assigned oversimplified distributions. Experimental work by the authors, however, has shown that the growth rate distribution in a vertical reactor cannot be successfully explained by reactant depletion alone.[9]

*Current address: Chevron Research Company, Richmond, CA 94802.

None of the previous studies of transport processes in silicon deposition reactors has taken into account the coupling of the transport equations for momentum, temperature and molar components, and the spatial distributions of these quantities in the reactor flow channel, which is characteristic of both the horizontal and the vertical cylinder reactors. In a recent paper, the authors[10] have demonstrated that transport processes in the vertical cylinder reactor occur under conditions of developing, laminar flow and that it is necessary to consider the coupled nature of the equations governing the transport of gas momentum, temperature, and reactant concentrations in both the radial and axial directions in the flow channel. In this paper, the problem of silicon deposition in the vertical cylinder reactor is formulated in terms of the coupled transport equations for momentum, heat, and mass transfer in developing laminar flow. Solutions to this system of simultaneous partial differential equations are obtained by computer calculations using a finite difference method. The numerical method takes into account the effects of a spatially varying inlet flow velocity, and the reactor geometry. The results of the computations are used to reveal the deposition rate distribution, the distributions of the gas velocity, temperature, and reactant concentrations in both the axial and radial directions of the flow channel.

THEORY

The vertical cylinder reactor is shown schematically in Fig. 1. The reactant gas mixture enters the quartz reactor chamber above the susceptor, flows over the susceptor, and exits at the bottom. The susceptor temperature is maintained at 1200°C by quartz heating lamps. Both the lamps and the outer wall of the reactor are cooled by a forced air cooling system. A summary of operating conditions is given in Table 1. The reactor design and dimensions as well as the operating conditions have been chosen to closely approximate those of an industrial reactor.[6] The eight-sided susceptor surface is idealized as the frustum of a cone, and gas flow in the reactor is considered to be axisymmetric. Since the Reynolds numbers for flow in the reactor are on the order of 10^2, and channel flow is known to be laminar for Reynolds numbers below 2000, the flow in the reactor is expected to be in the laminar regime. These assumptions simplify the mathematical problem to variation in two dimensions with cylindrical symmetry. Sugawara[11] has studied silicon deposition over a range of susceptor temperatures using a CVD apparatus with a rotating disk susceptor. His findings indicate that a transition from growth limited by kinetics to growth limited by diffusion occurs at about 1150°C. At 1200°C, deposition of silicon is controlled entirely by diffusion of the reactants to the susceptor surface.

The overall reactions for silicon deposition are the following:

$$SiCl_4 + 2H_2 \rightarrow Si(c) + 4\ HCl \qquad (1)$$

$$SiCl_4 + H_2 = SiCl_2 + 2HCl \ . \qquad (2)$$

Other side reactions are also known to occur, but the concentrations of reaction products are negligible, based on a study of the extensive thermodynamic calculations of Sirtl et al. for the Si-Cl-H System.[12] Their work shows that the efficiency η of the reaction of hydrogen with $SiCl_4$ to deposit silicon from a 1.15% $SiCl_4$ - 98.85% H_2 reactant gas at 1473°K is approximately 70%. The silicon molar deposition rate per unit area is thus 0.70 times the normal flux of $SiCl_4$ at the susceptor surface.

The equations governing transport processes and the relevant boundary conditions are summarized in Table 2 for steady, laminar, axisymmetric flow in the vertical cylinder reactor.[13] The transport equations are coupled by the presence or velocity terms in the energy and reactant mass continuity equations and by the dependence of the transport properties ρ, μ, k, C_p, and $\mathcal{D}_{ij}$ on the temperature and composition of the gas. The equations and methods used for evaluation of the transport coefficients are presented in the Appendix.

NUMERICAL COMPUTATION

A generalized, finite difference computer program was utilized for calculating the solutions to the coupled transport equations for momentum, temperature and molar concentrations.[14,15] The parabolic forms of the partial differential equations governing transport were reduced to six-point, finite difference form and then solved with a tri-diagonal matrix algorithm by a single-pass, marching integration through the finite difference grid of 42 by 220 points. As the marching integration proceeded downstream, the program assumed control of the grid points so that they were placed along lines enclosing constant mass flow. The downstream step size (distance between axial grid points) was controlled by a stability criterion within the program. The flow diagram for the computer program is shown in Fig. 2.

RESULTS AND DISCUSSION

The calculated velocity profiles within the flow channel of the reactor are shown in Fig. 3. The cross stream velocity profiles at different axial positions, shown in Fig. 3a, indicate that in the entrance region of the reactor, boundary layers develop at both walls of the flow channel to modify the initially uniform velocity profile. At a distance of about 13 cm from the channel entrance the boundary layers overlap, and a nearly parabolic velocity profile results. With increased downstream distance, the profile remains nearly parabolic, with the magnitude increasing as a consequence of thermal expansion in a channel of decreasing cross-sectional area. The velocity profiles differ from that expected for laminar flow in an annulus, because of the large thermal effects occuring near the susceptor. Because of

the large cross stream temperature gradient, volumetric expansion increases the velocity near the inner, or hot, wall of the channel.

The calculated results differ significantly from the velocity profile assumed by Eversteijn et al.[2,3] and other authors for the horizontal channel. The model of Eversteijn et al.[2,3] is not expected to give reasonable results over the first 18 cm of the susceptor because of the significant difference between the actual boundary layer shown by the present calculations and the boundary layer thickness (half the channel width) assumed by Eversteijn et al. Rundle's model[4,5], based on the assumption of laminar gas flow profile, is not reasonable below the leading edge of the susceptor. Shepherd's[1] assumption of a parabolic velocity profile, is seen to be in reasonable agreement with the calculated results only for the lower half of the flow channel. The flow regimes indicated by this study appear in Fig. 3b.

The temperature isotherms in the flow channel of the reactor are shown in Fig. 4. Heating of the gas appeared to occur rapidly in the first five centimeters of the reactor, while the variation of temperature across the gas stream became monotonically decreasing with radial distance at about fifteen centimeters from the top of the susceptor. In laminar flow, the temperature gradient across the gas stream remains large but is more evenly distributed at downstream positions.

Because of the large gradient near the leading edge of the susceptor, buoyancy forces on elements of fluid are expected to be large only in this vicinity. However, independent calculations indicate that the critical conditions for instability, namely $Gr/Re > 18$ is not met at an axial distance of only a few cm. Thus, the buoyancy forces can be expected to generate negligible reverse or upward velocity in the fluid near the susceptor surface. As the fluid is heated from the inlet temperature, the fluid velocity increases because of volumetric expansion. This effect further aids in suppressing reverse flow downstream from the leading edge region.

The calculated mean temperature of the gas within the flow channel is seen in Fig. 4 to increase rapidly near the leading edge of the susceptor. Therefore, the assumption of a uniform gas temperature is inappropriate in transport models of cold-wall reactors. In a previous theoretical analysis,[10] the authors show that the mean temperature in the flow channel of the reactor increases over a large portion of the susceptor. This phenomenon exerts a strong influence on the growth rate distribution, especially on the front part of the susceptor.

The concentration isotherms for the principal silicon species in the gas phase, $SiCl_4$, are shown in Fig. 5. The concentration gradient is largest at the susceptor surface near the leading edge of the susceptor, primarily owing to the large velocity gradient in

that region. However, the $SiCl_4$ concentration gradient is uniform over the majority of the susceptor surface, indicative of a uniform deposition rate.

The silicon epitaxial growth rate distribution is shown in Fig. 6 for Reynolds numbers of 50, 92.6, and 250. Growth rates calculated by the numerical method are initially higher than those predicted by the Developing Temperature Model.[10] The growth rates are shown in Fig. 6 to decrease with increasing downstream distance at a Reynolds number of 50, and to increase for a Reynolds number of 250. These results are consistent with the effect of the inlet velocity profile on the temperature distributions. Because the growth rate has a positive temperature dependence, the higher initial flow rates can be expected to cool the initial part of the susceptor, thereby reducing the growth rates below the values predicted by the numerical method. Yet the high velocity produces a larger molar concentration gradient at the susceptor surface, and a correspondingly higher deposition rate. On the other hand, for a low Reynolds number, the growth rate is high on the initial part of the susceptor, and reactant depletion is increased. Since deposition is high on the leading edge region, the reactant is depleted rapidly and downstream grown rates are lower.

As an example of the application of the finite difference method to process design calculations, a study was made of the effect of susceptor tilt angle on growth rate distribution. At a Reynolds number of 92.6, an outer reactor wall radius of 11.5 cm, and a mid-susceptor radius of 8.25 cm, growth rate distributions were calculated for susceptor tilt angles with tangents between 0.05625 and 0.0875. The results are shown in Fig. 7., These results showed that a susceptor tilt angle having a tangent of 0.08125 gave the most uniform growth rate distribution for Re = 92.6.

The tilting of the susceptor causes a decrease in the cross section of the flow channel with increasing downstream distance. As a consequence, both the mean flow velocity and the velocity gradient at the susceptor surface are increased. The effect of tilting the susceptor is thus to increase the deposition rates at large downstream distances and to reduce the growth rate in the leading edge region by reducing the rate of heating of the inlet gas.

CONCLUSION

The numerical calculation method allows detailed study of the velocity, temperature and molar concentration distributions in the flow channel of the vertical cylinder reactor. The results of the gas velocity calculations show that boundary layers develop on both walls of the flow channel over a significant length (18 cm at Re = 92.6) before overlapping. At the leading edge, a very steep thermal gradient occurs between the heated susceptor at 1473°K and the entering gas at

298°K. This steep gradient suggests the presence of a small region of upward flow near the susceptor leading edge due to strong upward buoyancy forces. Downstream, the average velocity of the gas increases on heating and the thermal gradient is distributed more evenly between the susceptor and the 773°K outer wall. The results of the $SiCl_4$ concentration calculations indicate a uniformly decreasing concentration gradient at the susceptor surface with increasing downstream distance. The growth rates in the reactor are shown to be influenced by the inlet gas flow rate and the susceptor tilt angle.

A major objective of reactor design is to develop large capacity reactors which can produce highly uniform deposition over all the substrates in the reactor, reproducible results from run to run, and an economical reactant consumption rate. The present method using numerical methods is extremely useful for developing insight into the silicon deposition process, for providing tests of conditions which optimize the reactor performance, and for providing a basis for scale-up of commercial reactors.

ACKNOWLEDGMENT

The financial assistance of the U.S. Energy Research and Development Administration and the Lawrence Berkeley Laboratory are gratefully acknowledged.

REFERENCES

1. W.H. Shepherd, J. Electrochem. Soc., 112, 988 (1965).
2. F.C. Eversteijn, P.J.W. Severin, C.H.J. van den Brekel and H.L. Peek, J. Electrochem. Soc., 117, 925 (1970).
3. F.C. Eversteijn and H.L. Peek, Philips Res. Repts., 25, 472 (1970).
4. P.C. Rundle, Int. J. Electron., 24, 405 (1968).
5. P.C. Rundle, J. Crystal Growth, 11, 6 (1971).
6. AMT 740 Reactor Manual, Applied Materials, Inc., Santa Clara, CA, 1975.
7. E. Fujii, H. Nakamura, K. Haruna and Y. Koga, J. Electrochem. Soc., 119, 8 (1972).
8. F.W. Dittman, Chemical Reactor Engineering II, H.M. Hulburt, ed., Advances in Chemistry Series 133, American Chemical Society, Washington, D.C., 1974, pp. 463-473.
9. C.W. Manke, Modeling of a Barrel Reactor for Chemical Vapor Deposition of Silicon, M.S. Thesis, University of California, Berkeley, 1976.
10. C.W. Manke and L.F. Donaghey, J. Electrochem. Soc., 124, 561 (1977).
11. K. Sugawara, J. Electrochem. Soc., 119, 326 (1970).
12. E. Sirtl, L.P. Hunt and D.H. Sawyer, J. Electrochem. Soc., 127, 7 (1974).
13. R.B. Bird, W.E. Stewart and E.N. Lightfoot, Transport Phenomena, John Wiley & Sons, Inc., New York, 1960.

14. D.B. Spalding, A General Program for Two Dimensional Boundary Layer Problems, Imperial College of Science and Technology, Department of Mechanical Engineering, Exhibition Road, London SW 7. Sept. 1973.

15. S.V. Pantankar and D.B. Spalding, Heat and Mass Transfer in Boundary Layers, 2nd Edition, London, Morgan-Grampian.

LIST OF SYMBOLS

C_p	heat capacity, J/(g-mole°K)
$\mathcal{D}$	diffusion coefficient, m^2/sec
G	linear growth rate, μ/min
k	thermal conductivity, J/(m-sec°K)
M_{Si}	molecular weight of silicon, 28 g/mole
p	pressure, atm (101.325 kPa)
r	radial distance, cm
r_i	inner radius, cm
r_o	outer radius, cm
R	gas constant, R = 82.06 atm-cm^3
Re	Reynolds number, $Re = \rho d_h v/\mu$
T	temperature, °K
T_i	inner wall temperature, °K
T_o	outer wall temperature, °K
v	velocity, cm/sec
x	axial distance, cm
X	mole fraction $SiCl_4$
X_i	mole fraction $SiCl_4$ at inner radius
z	axial distance, cm
α	thermal diffusivity = $k/(\rho C_p)$
μ	absolute viscosity, μ-poise
ρ	density, g/cm^3
$\Omega_{\mathcal{D}}$	collision integral for diffusion

APPENDIX

Transport Properties

Transport properties were determined for the pure components using experimental correlations and corresponding states methods. Properties of mixtures were then determined by empirical methods. Transport properties used in the calculations were determined with the following equations:

Viscosity (μpoise)

$$\mu_{H_2} = 88.0\ T^{0.6872} \exp\{-0.61732\ T^{-1} - 111.49\ T^{-2} - 3.9001\}$$

$$\mu_{SiCl_4} = \begin{cases} 0.5014\ T\ , & T < 760°K \\ 91.33[0.0090514\ T - 1.67]^{5/8}\ , & T > 760°K \end{cases}$$

$$\mu_{HCl} = \begin{cases} 18.794\ T^{3/2}/(T + 367.21)\ , & T < 700°K \\ 2.7827\ T^{0.7272}\ , & T > 700°K\ . \end{cases}$$

Heat Capacity ($J\ kg^{-1}{}^{\circ}K^{-1}$)

$$C_{P,H_2} = 14535 - 0.4023\ T + 9.816\times10^{-4}\ T^2$$

$$C_{P,SiCl_4} = 561.4 + 6.417\times10^{-2}\ T - 8.640\times10^{-6}\ T^2$$

$$C_{P,HCl} = 774.61 + 4.535\times10^{-2}\ T + 4.581\times10^{-5}\ T^2\ .$$

Thermal Conductivity ($J\ M^{-1}s^{-1}{}^{\circ}K^{-1}$)

$$k_{H_2} = 0.080796 + 3.7312\times10^{-4}\ T - 7.4683\times10^{-9}\ T^2$$

$$k_{SiCl_4} = c_{P,SiCl_4} + 61.18\ \mu_{SiCl_4}$$

$$k_{HCl} = \begin{cases} 2.104\times10^{-3} + 3.676\times10^{-5}\ T + 1.462\times10^{-8}\times T^2\ , & T < 700°K \\ 0.9661(c_{P,HCl} + 285.1)\mu_{HCl}\ . \end{cases}$$

Binary Diffusion Coefficients ($m^2 s^{-1}$)

$$\mathcal{D}_{SiCl_4-H_2} = 7.0861\times10^{-9} T^{3/2}/\Omega_{\mathcal{D}}$$

$$\sigma = 4.31 \text{ Å}$$

$$\varepsilon/k = 144°K$$

$$\mathcal{D}_{HCl-H_2} = 1.4196\times10^{-8} T^{3/2}/\Omega_{\mathcal{D}}$$

$$\sigma = 3.083 \text{ Å}$$

$$\varepsilon/k = 143°K$$

where

$$\Omega_{\mathcal{D}} = \frac{6.7928}{T_r} + \frac{0.1930}{\exp(0.47635\ T_r)} + \frac{1.03587}{\exp(1.52996\ T_r)} + \frac{1.76474}{\exp(3.89411\ T_r)}, \quad T_r = kT/\varepsilon .$$

Mixtures:

The viscosity of the gaseous mixture was determined by Wilke's method (*). The mixture density of the mixture was calculated according to the ideal gas law. The heat capacity of the mixture was determined by adding the component heat capacities weighted by their mole fractions. The mixture thermal conductivity was obtained from the Mason and Saxena formulation of the Wassiljewa equation (†).

*C.R. Wilke, J. Chem. Phys., 18, 517 (1950).

†E.A. Mason and S.C. Saxena, Phys. Fluids, 1, 361 (1958).

Table 1

Typical Operating Conditions for Silicon Deposition

Variable	Values
Temperature	Inlet: 298°K;Susceptor: 1473°K,Outer wall: 773°K.
Pressure	1 atm (101325 Pa)
$SiCl_4$ mole fraction	Inlet: 0.0115.
H_2 mole fraction	Inlet: 0.9885.
Susceptor dimensions	Length: 40cm;Mean inner radius: 8.25cm; Outer radius: 11.5cm;Tilt angle: 3.58°.
Reynolds number	92.6 (mean value).

Table 2
Transport Equations, Boundary Conditions, and Initial Values

Momentum Equation, axial direction $\rho u \frac{\partial u}{\partial x} = \frac{1}{r} \frac{\partial}{\partial r} \left(\mu r \frac{\partial u}{\partial r} \right) - \frac{dP}{dx}$	Boundary Conditions: $u = 0, \quad r = r_i$ $u = 0, \quad r = r_o$
Initial Value: $u = u_{inlet}, \quad z = 0, \quad r_i < r < r_o$	
Energy Equation, axial direction $\rho u \frac{\partial \tilde{h}}{\partial x} = \frac{1}{r} \frac{\partial}{\partial r} r \left(\frac{k}{C_p} \frac{\partial h}{\partial r} - u \tau \right)$ where $\tilde{h} = h + u^2/2$ and $h = C_p T$.	Boundary Conditions: $T = 1473^{o}K, \quad r = r_i$ $T = 773^{o}K, \quad r = r_o$
Initial Value: $T = 298\ ^{o}K, \quad z = 0, \quad r_i < r < r_o$	
Equation for Mass Continuity of $SiCl_4$ $\rho u \frac{\partial X_i}{\partial x} = - \frac{1}{r} \frac{\partial}{\partial r} \left(r \rho D_{i-H_2} \frac{dX_i}{dr} \right)$	Boundary Conditions: $X_i = 0, \quad r = r_i$ $\frac{\partial X_i}{\partial r} = 0, \quad r = r_o$
Initial Condition: $X_i = .0115, \quad z = 0, \quad r_i < r \leq r_o$	
Equation for Mass Continuity of HCl $\rho u \frac{\partial X_j}{\partial x} = - \frac{1}{r} \frac{\partial}{\partial r} \left(r \rho D_{j-H_2} \frac{dX_j}{dr} \right)$	Boundary Conditions: $\frac{\partial X_j}{\partial r} = -4 \frac{\partial X_i}{\partial r}, \quad r = r_i$ $\frac{\partial X_j}{\partial r} = 0, \quad r = r_o$
Initial Condition: $X_j = 0, \quad z = 0, \quad r_i < r \leq r_o$	

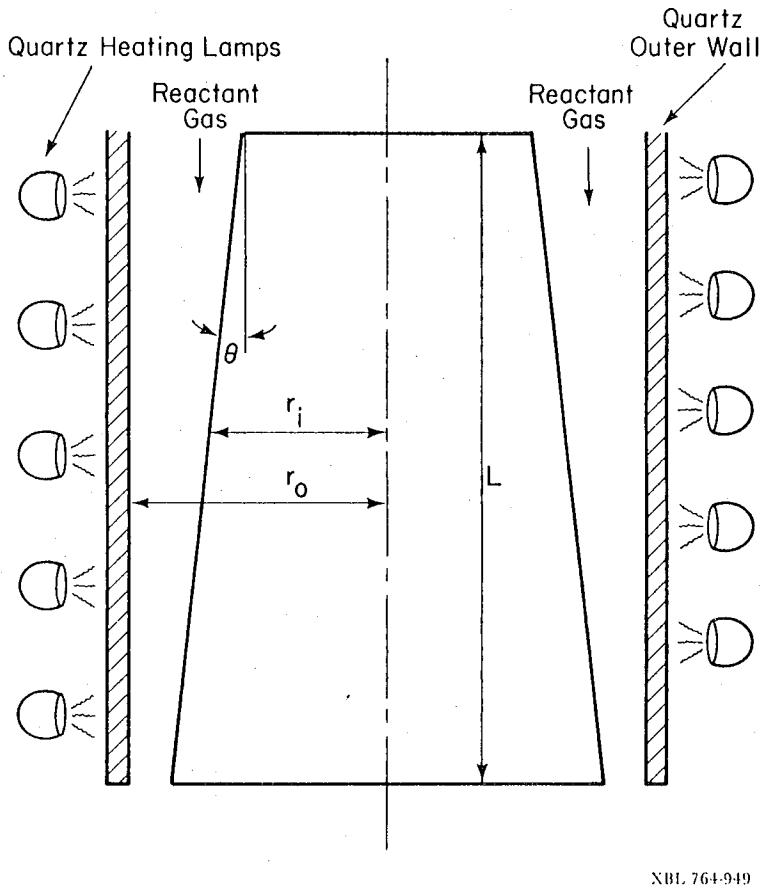

Figure 1. The vertical cylinder reactor cross section.

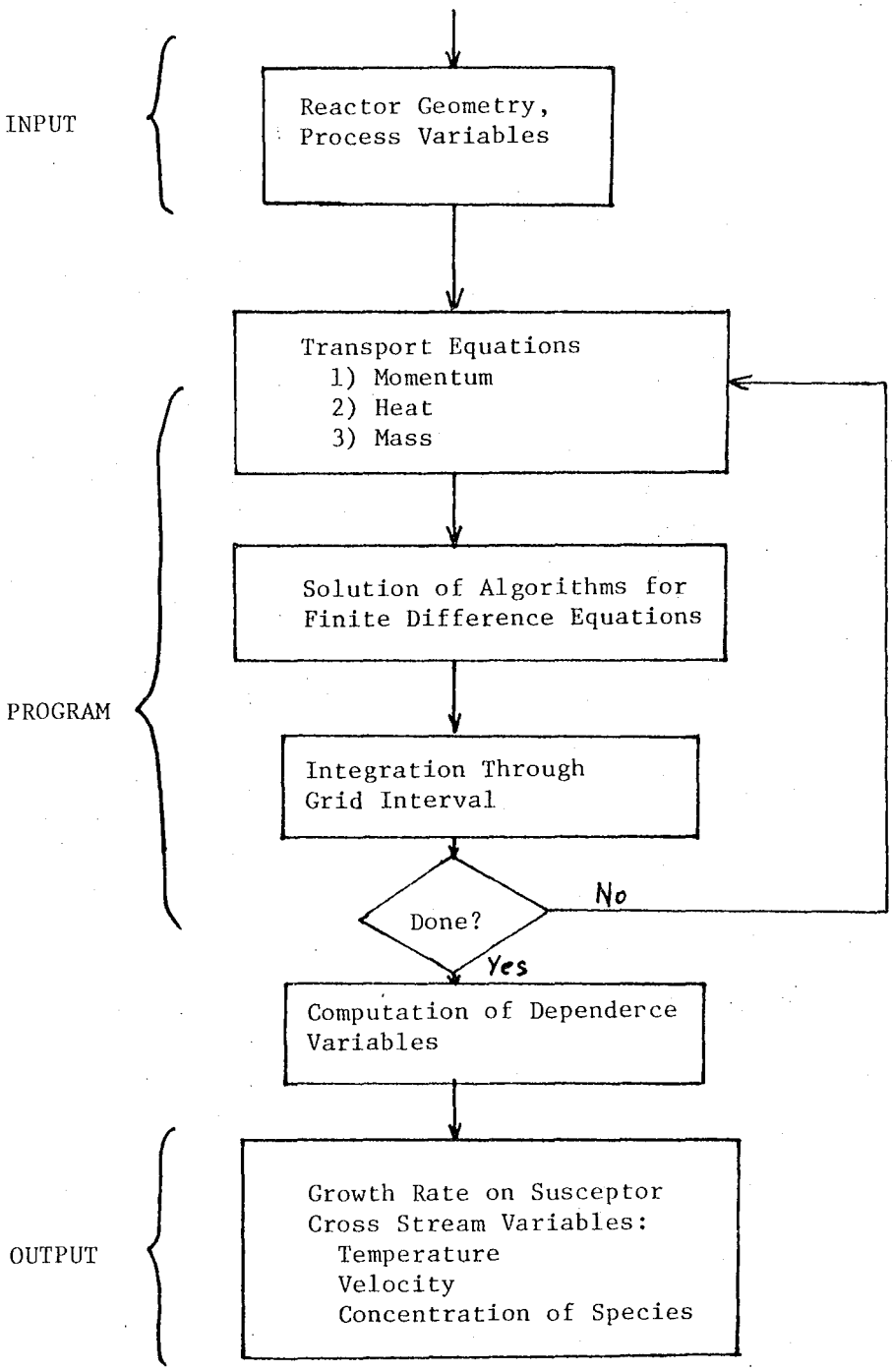

Figure 2

Block diagram of the computer simulation program

XBL 777-9554

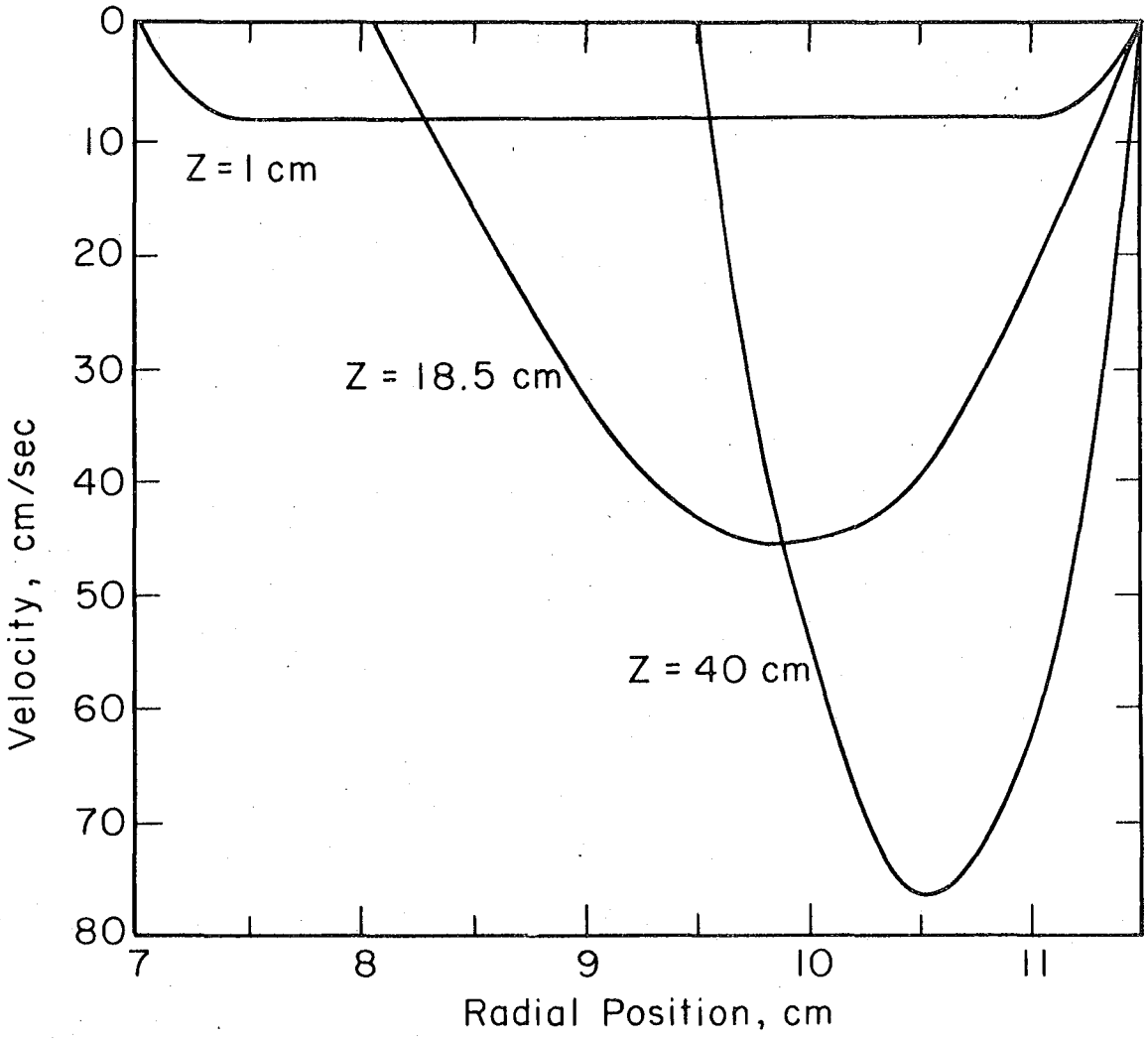

(a)

Z = 1 cm :	boundary layer	uniform velocity profile	boundary layer
Z = 18.5 cm		Boundary layers from both side walls overlap	
Z = 40 cm		Fully developed, quasi-parabolic velocity profile	

(b)

Figure 3. Velocity profiles within the vertical cylinder reactor: (a) cross stream velocity profiles; (b) flow regimes.

XBL 776-9544

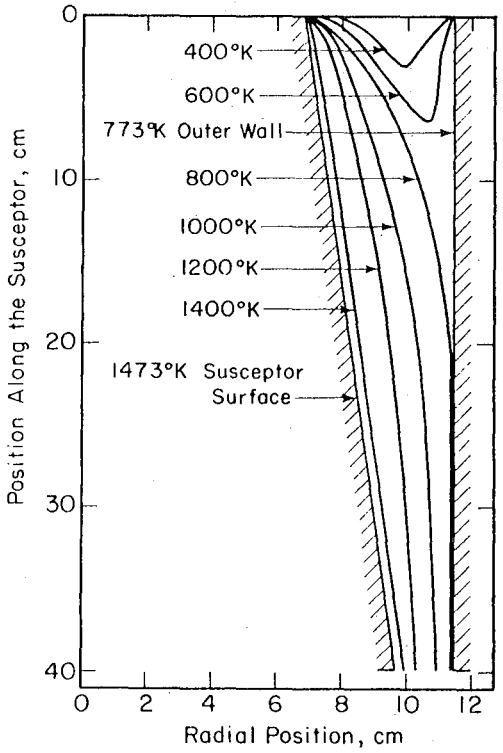

Figure 4. Temperature isotherms within the flow channel.

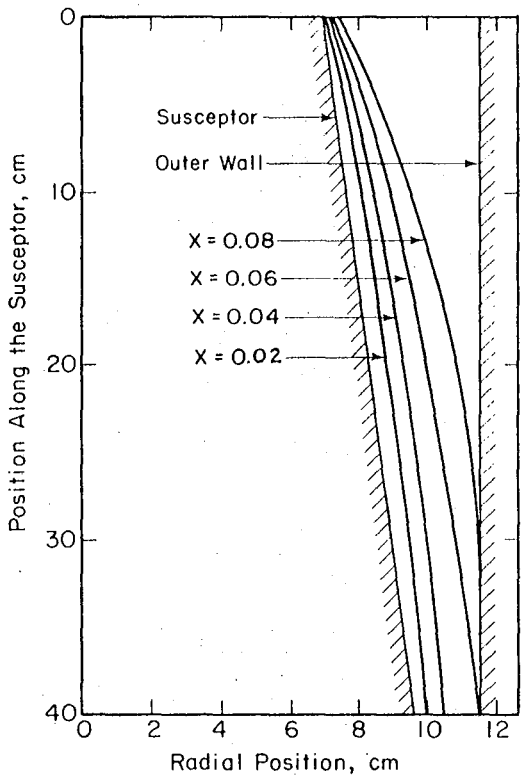

Figure 5. Isoconcentration curves for SiCl$_4$ within the flow channel of the reactor.

XBL 776-9557

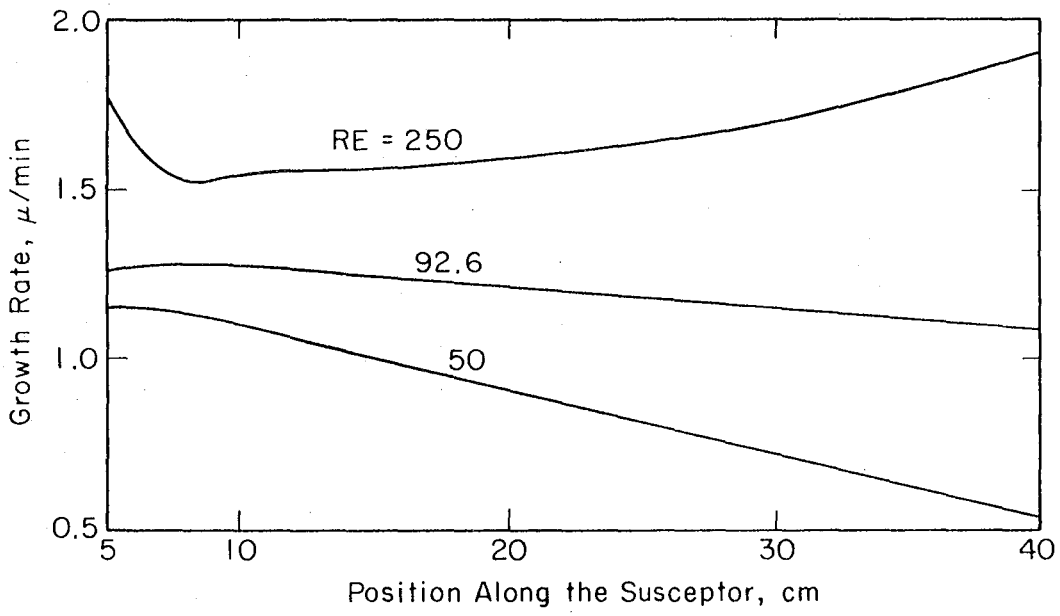

Figure 6. Axial variation of the growth rate for fixed inlet flow rates.

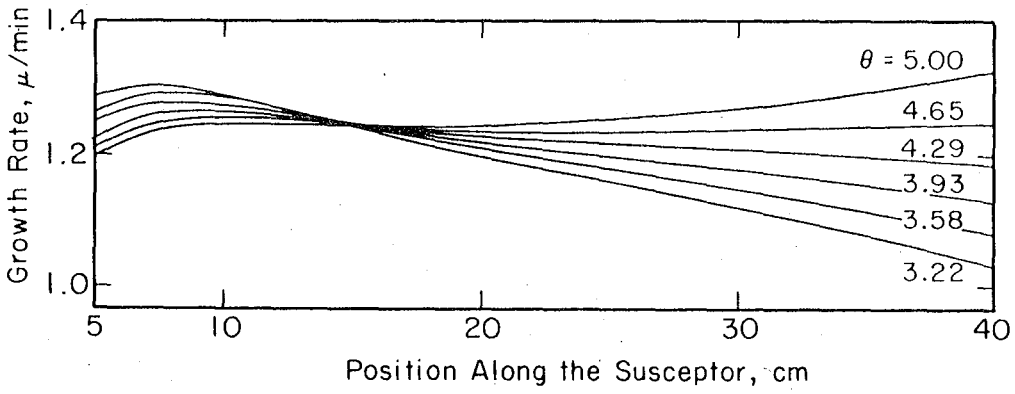

Figure 7. Axial variation of the growth rate for different susceptor tilt angles.

XBL 776-9551

This report was done with support from the United States Energy Research and Development Administration. Any conclusions or opinions expressed in this report represent solely those of the author(s) and not necessarily those of The Regents of the University of California, the Lawrence Berkeley Laboratory or the United States Energy Research and Development Administration.